Available online at www.sciencedirect.com

ScienceDirect

Ciência & Tecnologia dos Materiais 29 (2017) e82–e86

http://ees.elsevier.com/ctmat

Special Issue "Materiais 2015"

Microstructure and mechanical properties of Al/SiC composite surface layer produced by friction stir processing

C.M. Abreu[a], R. Acuña[a,*], M. Cabeza[a], M.J. Cristóbal[a], P. Merino[a], D. Verdera[b]

[a]*Department of Materials Science, University of Vigo, 36310 Vigo, Spain*
[b]*Technologival Centre AIMEN, Relva 27A, 36410, O Porriño, Pontevedra, Spain*

Abstract

Metal matrix composites (MMCs) are a new class of materials that exhibit good wear resistance and high hardness. Since the wear resistance and hardness are surface properties, if the reinforcing particles are only added to the surface layer instead of bulk, the wear resistance and surface hardness can be improved without sacrificing the bulk properties.
In this study, was attempted to incorporate micro-sized SiC particles into an AA2024-T351 aluminium alloy by a friction stir processing (FSP) to form surface composite layer. The SiC particles (average particle size of 22.7 µm) were packed into a groove of 1.5 mm width and 1.5 mm depth cut on the aluminium plate. The influence to probe several strategies for reinforcement (number and direction of passes) on the particle distribution and homogeneity was studied.
Microstructural observations were carried out by employing both optical and scanning electron microscopy. In addition, the Electron Backscatter Diffraction (EBSD) technique was used to obtain crystallographic data as crystal orientation, grain size distribution and texture. The results have confirmed the refinement of grain produced in the nugget region of the processed alloy. On the other hand, although there is not an increase of hardness, surface composite layer presents better wear resistance than the aluminium base alloy as indicated by a lower specific wear rate (27%).

Keywords: Friction stir processing; AA2024-T351; SiC; EBSD; mechanical and tribological properties.

1. Introduction

Recently, much attention has been paid to the friction stir processing (FSP) for composite manufacturing [1-3]. That FSP tool can be used to distribute ceramic particles as reinforcement on the surface of light metals like aluminium or magnesium alloys. Compared with unreinforced metals, the metal-matrix composites reinforced with ceramic particles exhibit high strength, high elastic modulus, and improved resistance to wear, creep and fatigue, which make them promising structural materials for aerospace and automobile industries.
Several studies [4,5] have investigated the effect of the processing parameters on microstructure and mechanical properties on the Al/SiC surface composites. The present investigation shows the microstructural results (defects, particle distribution and grain structure) and the mechanical and tribological properties obtained, using a single tool with different conditions testing, under the same process parameters to incorporate micro-sized SiC particles in the AA2024-T351 alloy to form a composite surface layer.

2. Experimental Procedure

This study has been carried out in a commercially available aluminium alloy (AA2024-T351) whose chemical composition is (wt.%): 4.57Cu, 1.5Mg, 0.65Mn, 0.12Fe, 0.07Si, 0.06Zn, 0.04Ti, 0.01Cr, Al balance. The sheet of 5 mm thick was manufactured

* Corresponding author.
E-mail *address:* robertoacua@gmail.com (R. Acuña)

http://dx.doi.org/10.1016/j.ctmat.2016.07.001

by hot-and-cold rolling. The SiC particles used to reinforce the surface has a purity of 99.0% and average particle size of 22.7 μm. Based on preliminary trials, tests were conducted packing the SiC reinforcement particles into a groove with a square section of 1.5 mm width × 1.5 mm depth and a length of 350 mm. The groove was made in a straight line along the middle length of each aluminium work pieces. The pin of the tool was positioned centred in the machined groove.

FSP tests were performed in a machine MTS PDS-4 Intelligent-Stir using a MP159 tool with a conical threaded pin and a threaded shoulder, whose dimensions are: shoulder diameter = 12 mm, pin diameters = 4-5 mm and pin length = 1.8 mm.

For aluminium alloy 2024, FSP tests were performed under position control, at a constant rotation speed of 1000 rpm and a traverse speed of 300 mm/min. The tool was set perpendicular to the fixed substrate with a tilt angle of 1.5º and the depth of penetration was set at 1.9 mm.

The reinforcement strategy was based on performing three different conditions: condition 1 (one FSP single pass), condition 2 (two FSP passes along the opposite direction), and condition 3 (two FSP passes along the same direction).

The distribution of SiC particles was characterized by optical microscopy (OM).

Electron Backscatter Diffraction (EBSD) was used to provide crystallography information at very specific points in a sample. The information obtained from Kikuchi patterns is represented in the form of maps, getting maps of the crystallographic texture or crystal orientation (Euler angles, inverse pole figures ...), grain size maps, band contrast, etc.. The samples were polished finish up with a 0.05 μm colloidal silica solution. The specimen tilt angle was 70º and the used step sizes were 0.5 and 0.05 μm in the base material (BM) and in the nugget, respectively. It was considered as grain boundary when the misorientation angle was greater than 10°.

Vickers microhardness of the surface and cross section of the BM and the processed zone (PZ) were also measured. PZ is formed by the nugget and the TMAZ (Thermo-Mechanically Affected Zone). A 200 gf load indent was used.

Sliding wear experiments were performed in the mode “pin-on-disk” applying a load of 20 N. The pin used was a 4 mm diameter of alumina. Tested samples were rotated at 200 rpm. Wear track radius was 3 mm and the sliding distance was 500 m.

Wear tracks were characterized by both optical and SEM microscopy to assess wears mechanisms.

3. Results and Discussion

3.1. Characterization of processed samples

The surface appearance of the PZ with a FSP single pass (condition 1) is good (Fig. 1), presenting small burrs at the edges. As it is shown in Fig. 1, the distribution of particles in the PZ is quite homogeneous, except for a small concentration of particles on the retreating side.

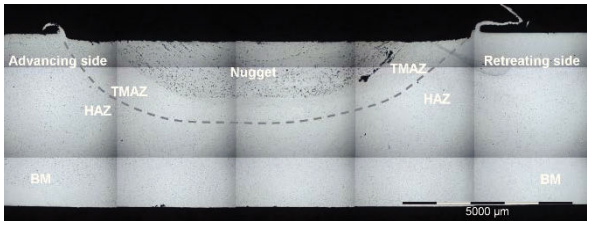

Fig. 1. Cross section of the alloy processed with the condition 1.

The condition 2 presents an irregular surface appearance. Moreover, in the retreating side, a higher concentration of particles is observed since the tool tends to sweep the particles, accumulating them in this region, as depicted in Fig. 2. Furthermore, close observation of the outermost region of this cross section shows a significant accumulation of particles on advancing side.

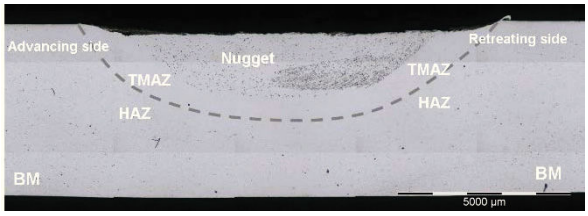

Fig. 2. Cross section of the alloy processed with the condition 2.

Finally, the condition 3 shows a good surface appearance similar to obtained in condition 1. However, it is observed the presence of burrs on the edges of the PZ due to a slight increase in the tool penetration. As it could be observed in Fig. 3, the SiC particles are distributed homogeneously inside the nugget zone without any defects, showing a good bonding between the SiC particles and Al matrix alloy.

Particle count performed on the sample in condition 3 gives the following results: a density of 200 part./mm^2 in the surface zone with a mean particle diameter of

4.5 µm, and a density of 126 part./mm^2 in a cross section with a mean particle diameter of 7.8 µm.

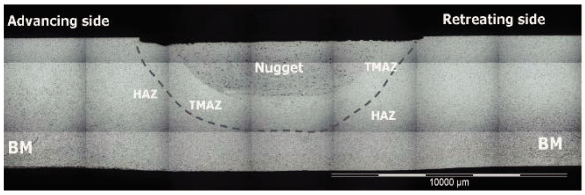

Fig. 3. Cross section of the alloy processed with the condition 3.

These results indicate that the stir process has produced a fracture effect in the particles.
Consequently, taking account that the best distribution of particles corresponds to the condition 3 (two FSP passes along the same direction), the rest of this study was focused only on this condition.

3.2. Microstructural characterization by EBSD

Figs. 4 and 5 show the selected zone in the BM and in the nugget region, respectively, to obtain the Electron Backscatter Diffraction Patterns. The BM and nugget presented an indexed rate of 73% and 67%, respectively.

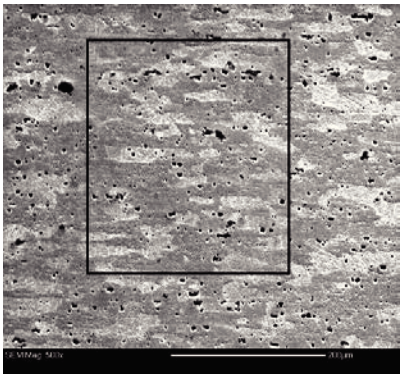

Fig. 4. SEM image of selected zone in BM.

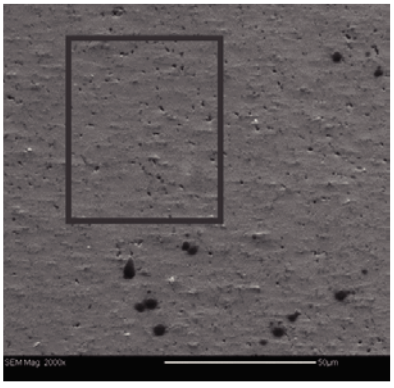

Fig. 5. SEM image of the nugget.

Figs. 6 and 7 present the inverse pole figures (IPF) maps of the BM and nugget region in which the colours correspond to the crystal orientations. Fig. 8 shows the colour map for displaying the map of IPF, where the red, green and blue colours are assigned to grains whose <001>, <101> or <111> axes, respectively, are parallel to the direction of projection of the IPF (typically, the normal direction to the surface). IPF maps give information of the crystalline orientation of each of the analysed grains [6].

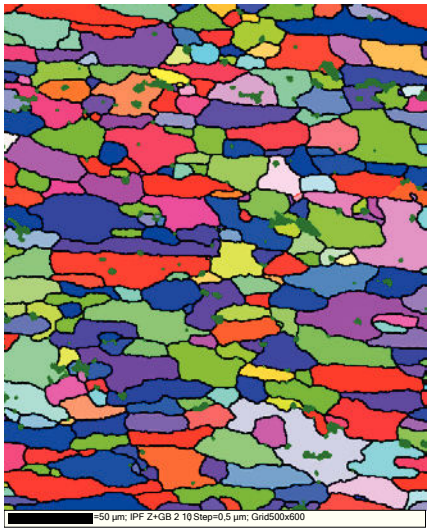

Fig. 6. IPF map of the BM.

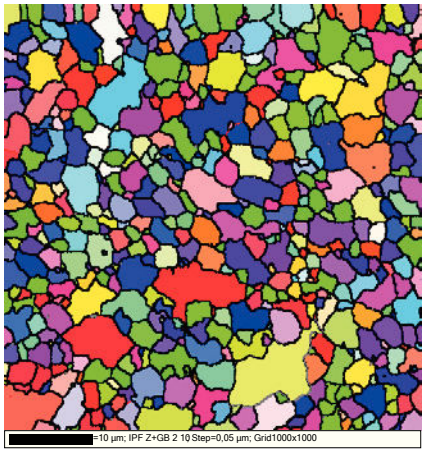

Fig. 7. IPF map of the nugget region.

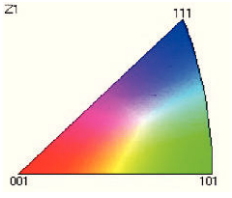

Fig. 8. IPF color map.

The analysis of the previous images indicate a grain refinement of the aluminium alloy matrix in the nugget region in comparison with the BM. The average grain size in the BM is 14 μm with a total of 227 grains counted, while in the nugget is 2 μm with a total of 503 grains counted. As can be seen in the tables of grain size distribution, the grain size in the BM is greater compared to the nugget (Table 1). According to several researchers [7-8] this grain refinement in the nugget is due to the large plastic deformation together with the temperature increase produced by the whipping of material during friction stir process, causing dynamic recrystallization of the material.

Table 1. Grain size distribution from BM and nugget.

D_{av} (μm)	BM	D_{av} (μm)	Nugget
≤ 8	31%	≤ 2	66%
$8 < D_{av} \leq 16$	35%	$2 < D_{av} \leq 4$	28%
$16 < D_{av} \leq 24$	17%	$4 < D_{av} \leq 6$	5%
$D_{av} > 24$	17%	$D_{av} > 6$	1%

3.3. Microhardness

Fig. 9 illustrates the microhardness profiles along the cross section of the processed sample; these values have been determined at intervals of about 0.6 mm. The blue line represents the hardness values obtained at the top and the pink line at the bottom of the cross section sample. Fig. 10 shows the microhardness values obtained across the surface of the processed alloy, under the same condition of Fig. 9. The selected area (brown) corresponds to the region where the SiC particles are incorporated.

The obtained average microhardness along the cross section (Fig. 9) are: 138HV0.2 in the BM, 122HV0.2 in the TMAZ/HAZ (Heat Affected Zone) and 139HV0.2 in the PZ (nugget and/or TMAZ) at the upper line, and 121HV0.2 in the TMAZ/HAZ at the lower line. The obtained surface average microhardness (Fig. 10) are: 140HV0.2 in the BM, 127HV0.2 in the TMAZ/HAZ and 142HV0.2 in PZ.

As it can be seen in Figs. 9 and 10, the hardness of the TMAZ/HAZ displayed a significant decrease compared to that of the base material. This can be justified due to the loss of precipitation hardening consequence to the T351 temper. Other researchers have observed similar results on a friction stir welding of AA2024-T351 alloy [9]. The results of their research show that in this softened region (TMAZ/HAZ), most of the hardening precipitates (GP zones) were transformed to incoherent S-phase as a result of rising temperatures due to FSP.

On the other hand, in PZ region the hardness values are similar to the BM. In this region, where the precipitation hardening has been lost as well as in TMAZ/HAZ region, the higher hardness values are due to the refinement of grain structure by dynamically recrystallization and the presence of fine SiC particles.

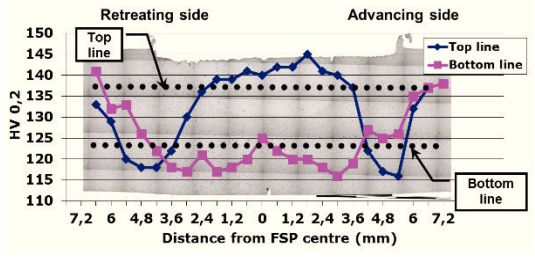

Fig. 9. The variation in microhardness along the cross section of the processed alloy.

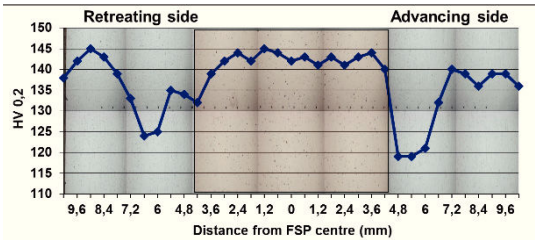

Fig. 10. The variation in microhardness along the surface of the processed alloy.

3.4. Tribological properties

In Fig. 11, a comparative graph of friction coefficient at steady-state between BM and PZ is shown. These results show a decrease of the friction coefficient in the PZ (0.37) in comparison to the BM (0.45). In both cases the evolution of the friction coefficient and its fluctuations is the same. In both tests occurs a release of a large amount of particles. In BM, the particles correspond to the aluminium matrix, while in the PZ those particles are a mix of aluminium and SiC ceramic particles. The presence of wear particles (debris) is indicative that the predominant mechanism of wear is abrasive. Moreover, the study of wear tracks shows that the surface of the groove is largely covered by wear particles that are crushed during the passage of the pin, forming a new surface wear; thus the predominant sliding wear mechanism at the end of the test is the adhesive, as shown in the SEM images obtained from the tracks at the end of the wear test (Figs. 12 and 13).

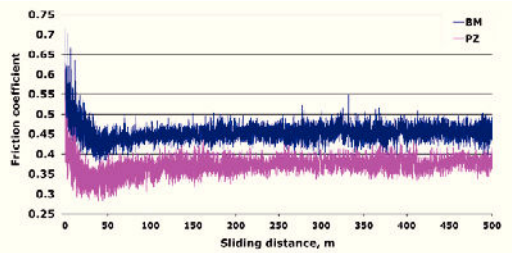

Fig. 11. Comparative graph of friction coefficient variation as a function of distance between BM and PZ.

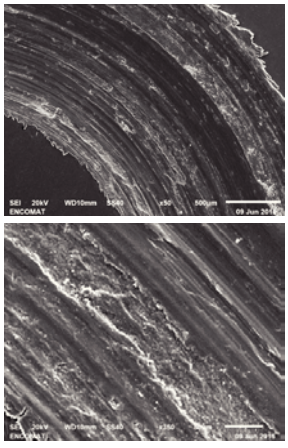

Fig. 12. SEM micrographs of wear track on the BM.

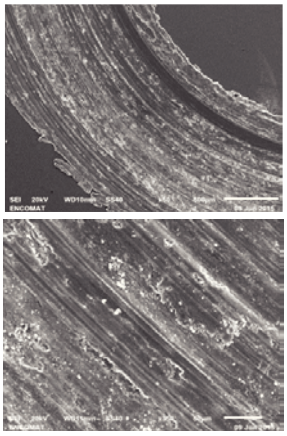

Fig. 13. SEM micrographs of wear track on the nugget region.

Although the specific wear rate on the surface of the processed zone ($2.64x10^{-4}$ mm^3/Nm) is slightly lower than that obtained on the surface of BM ($3.63x10^{-4}$ mm^3/Nm), there are notable differences in the morphology of the wear track. In the PZ the wear track has a depth of 143 µm and a width of 1457 µm, while the BM depth is 168 µm and the width is 1654 µm. Therefore, due to the addition of the ceramic particles of SiC and although the surface hardness of the material in the PZ is almost the same as in the BM, a shallow and less wide wear track than in BM is produced. These results indicate that the PZ undergoes lower plastic deformation.

4. Conclusions

– Under the parameters used in this study and the selected tool, the more uniform distribution together with a lower concentration of the SiC particles was obtained using two FSP passes in the same direction;

– EBDS analysis shows a significant grain refinement of the aluminium matrix in the nugget region that is due to dynamic recrystallization of the matrix during the stirring of the material;

– The nugget region do not exhibit a measurable increased hardness because there is a loss of precipitation hardening of the alloy in the T351 temper as a result of rising temperatures due to FSP. Additionally, for the same reason, the TMAZ and HAZ regions, where there are no embedded particles, present a significant hardness loss;

– Wear sliding tests show that surface composite layer presents better wear resistance than the aluminium base alloy as indicates the lower friction coefficient together with a lower specific wear rate (27%).

Acknowledgements

The authors wish to acknowledge the Ministry of Economy and Competitiveness for the financial support under project: MAT2013-48483-C2-2-P.

References

[1] R.S. Mishra, P.S. De, N. Kumar, Friction Stir Welding and Processing, Springer International Publishing, Switzerland, 2014.
[2] J. Gandra, R. Miranda, P. Vilaça¸ A. Velhinho, J. Pamies Teixeira, J. Mater. Process. Technol. 211 (2011) 1659.
[3] S. Sahraeinejad, H. Izadi, M. Haghshenas, A.P. Gerlich. Mater. Sci. Eng., A 626 (2015) 505.
[4] A. Devaraju, A. Kumar, B. Kotiveerachari, Mater. Des. 45 (2013) 576.
[5] Mojtaba Salehi, Hamidreza Farnoush, Jamshid Aghazadeh Mohandesi, Mater. Des. 63 (2014) 419.
[6] V. Randle, Microtexture Determination and its Applications, 2nd ed., Maney Publishing, London, 2008.
[7] R.W. Fonda, J.F. Bingert, K.J. Colligan, Scr. Mater. 51 (2004) 243.
[8] R.W. Fonda, K.E. Knipling, K.J. Colligan, Scr. Mater. 58 (2007) 343.
[9] C. Genevois, A. Deschamps, A. Denquin, B. Doisneau-Cottignies, Acta Mater. 53 (2005) 2447.